**Title**
WAVELENGTH MODULATION SPECTRA AND BAND STRUCTURES OF InP AND GaP



**Author**
De Alvarez, Carmen Varea.

**Publication Date**
1972

Submitted to Physical Review



LBL-479
Preprint



# WAVELENGTH MODULATION SPECTRA AND BAND STRUCTURES OF InP AND GaP

Carmen Varea de Alvarez, John P. Walter,
Marvin L. Cohen, J. Stokes and Y. R. Shen

January 1972

AEC Contract No. W-7405-eng-48



## DISCLAIMER

# Wavelength Modulation Spectra and Band Structures of InP and GaP

Carmen Varea de Alvarez*†, John P. Walter*‡, Marvin L. Cohen*,

J. Stokes and Y. R. Shen

Department of Physics, University of California

and

Inorganic Materials Research Division, Lawrence Berkeley Laboratory

Berkeley, California 94720

## Abstract

Modulated reflectivity measurements of InP and GaP at 5 , 77 , and 300°K are compared with empirical pseudopotential calculations of the electronic band structure, the imaginary part of the frequency-dependent dielectric function, the reflectivity, and the derivative of the reflectivity.

*Supported in part by the National Science Foundation Grant GP 13632.

†Consejo Nac. de Ciencia y Tecnología Fellowship, México.

‡Present address, Department of Physics, Brandeis University, Waltham, Massachusetts 02154.

## I Introduction

Modulated reflectivity measurements have become one of the most accurate methods for the determination of critical points in the band structure of diamond and zincblende type semiconductors. Semi-empirical calculations using the data these experiments provide have been highly successful in describing the electronic structure of these materials.[1,2] In this paper we combine these techniques to study InP and GaP.

The modulated reflectivity measurements for cubic InP and GaP crystals were measured at 5 , 77 , and 300°K. The results appear in Figs. 1 and 2 and the experimental procedure is described in the next section. Using the experimental data at 5°K we have obtained the band structure of InP using the empirical pseudopotential method[1]. We have also calculated the imaginary part of the frequency-dependent dielectric function $\epsilon_2(\omega)$, the reflectivity $R(\omega)$ and the modulated reflectivity spectra $R'(\omega)/R(\omega)$ which are compared directly with experiment. Spin-orbit corrections in InP are small and are not included; their effects are discussed by comparison with other zincblende crystals.

We have made an analysis of the critical points of the calculated optical structure to identify the interband transitions responsible for the prominent peaks. We also compare our $R'(\omega)/R(\omega)$ experimental curve for GaP with an earlier theoretical calculation by J. P. Walter and M. L. Cohen,[4] and we include here for completeness their analysis of the critical point structure for this crystal. The calculated optical properties for both InP and GaP agree reasonably well with experiment.

To study the indirect energy differences we have concentrated on the $\Gamma_{15} - X_1$ gap for InP and GaP using experimental data[5] on the $In_{(1-x)}\,Ga_{(x)}P$ ternary alloys. For GaP, the Walter and Cohen results for the $\Gamma_{15} - X_1$ gap agrees reasonably well with experiment. For InP, we have had to introduce an effective mass correction to fit our calculated value to the $\Gamma_{15} - X_1$ experimental gap on the InP side of the ternary. The direct gaps are not affected by this correction.

## II Experimental Procedure and Results

The logarithmic derivatives of the reflectivity spectra of GaP and InP were measured using a wavelength-modulation spectrometer. Construction and operation of the spectrometer have been described earlier[6]. The spectral resolution was chosen to be around 50 Å. The spectra of GaP and InP were recorded in the range from 2 to 6 eV at three different temperatures, 5 , 77 , and 300°K. The temperature control has a long-term stability of less than 1°K/hr.

Single crystals of GaP and InP were kindly provided by Dr. L. M. Foster of IBM Research Laboratory, Yorktown Heights. The GaP sample was vapor grown in a $PCl_3$ system on a GaAs substrate, which was later removed. The growth was on the (1, 1, 1) face. The sample has a conductivity of $10^{-8}$ $cm^{-1}$ and is believed to be very pure. For the reflectivity measurements, the front surface of the sample was mechanically polished and then chemically etched in a 1:1 solution of HCl and $HNO_3$ for two minutes.[7] In order to eliminate the effect of reflection from the back surface of the sample in the low absorption region, the back surface was ground and painted black.

The modulated reflectivity spectra of GaP and InP when compared with the corresponding thermoreflectance[9] and electroreflectance[10,11] spectra show more fine structure, especially at low temperature and in the higher frequency region. Shaklee and Rowe[12] have previously reported the wavelength-modulation spectra of InP at room and liquid $N_2$ temperatures in the spectral region between 2.8 and 3.5 eV. Their results are in good agreement with ours.

Our derivative spectra of GaP and InP have close similarity to those of the other semiconductors with zincblende structure.[6] Following the notation of Cardona et al.[11], we can divide the structure in each spectrum into groups, labelled by $E_0$, $E_1$, $E_2$, $E_0'$, $E_1'$, etc. It is believed that in different semiconductors, the same group results from optical transitions in the same general area of their band structures. This has been confirmed by detailed pseudopotential calculations as we shall see later.

## III Calculations

In applying the EPM to obtain the electronic band structure for InP, we have used the pseudopotential Hamiltonian

$$H = -\frac{\hbar^2}{2m}\nabla^2 + V(\vec{r}) \qquad (1)$$

where the weak local pseudopotential $V(\vec{r})$ is taken to be a superposition of spherical atomic pseudopotentials around the In and P atoms.

The potential $V(\vec{r})$ is expanded in reciprocal lattice vectors and for convenience expressed in terms of a symmetric and antisymmetric part giving

$$V(\vec{r}) = \sum_G [V^S(|G|)\cos\vec{G}\cdot\vec{\tau} + iV^A(|G|)\sin\vec{G}\cdot\vec{\tau}]e^{-i\vec{G}\cdot\vec{r}} \qquad (2)$$

where $\vec{\tau} = \frac{1}{8} a(1,1,1)$, a is the lattice constant. Since the pseudopotential is weak we are making the approximation $V(|G|) = 0$ for $G^2 >> 12$ and the only form factors which enter in the calculation are $V^S(\sqrt{3})$, $V^S(\sqrt{8})$, $V^S(\sqrt{11})$, $V^A(\sqrt{3})$, $V^A(2)$, and $V^A(\sqrt{11})$.

Using as our starting point the six form factors given by Cohen and Bergstresser,[13] we have calculated the band structure at many points in the Brillouin zone. With these values of $E(\vec{k})$ and the calculated dipole matrix elements we have calculated the imaginary part of the dielectric function. This calculation is described by Walter and Cohen[3,4], in which $\epsilon_2(\omega)$ is obtained at low energies assuming transitions between the three highest valence bands and the 6 lowest conduction bands. A tail function of the form $\beta\omega/(\omega^2 + \gamma^2)^2$ is used at high energies to take into account high energy transitions. This tail function starts at 8.3 eV, $\beta$ is determined from continuity and $\gamma = 4.5$. From $\epsilon_2(\omega)$ the real part of the dielectric function is obtained by a Kramers-Kronig transformation and from these two functions we obtain the reflectivity $R(\omega)$ and the modulated reflectivity $R'(\omega)/R(\omega)$. The theoretical $R'(\omega)/R(\omega)$ curve obtained from Cohen and Bergstresser pseudopotential form factors showed the same main structures as the experimental curve; thus the most important identifications were easily made.

In order to get better agreement with experiment, the main structure observed in the reflectivity curve has been shifted. The method of adjusting the values of the form factors has been described by Walter and Cohen.[3,4] Our pseudopotential form factors obtained after several iterations were (in Ry)

$V_3^S = -0.2704$ , $V_8^S = 0.0345$ , $V_{11}^S = 0.0442$ ,

$V_3^A = 0.0888$ , $V_4^A = 0.054$ , and $V_{11}^A = 0.0327$ .

These values yield a good fit to the modulated reflectivity at 5°K. The lattice constant is 5.862 A.

To determine the transitions responsible for structure in the $\epsilon_2(\omega)$ curve we first find the energy of a particular peak. From our tabulated interband contributions to $\epsilon_2(\omega)$ we are then able to determine which interband transition gives rise to the main contribution to this peak or shoulder. Once the interband transition has been identified we determine where in the Brillouin zone a critical point appears with the required energy difference and large oscillator strength. The final proof that our identification is correct is made by varying the form factors by a small amount and observing the change in the energy gap, because the energy change for the chosen transition should be the same as the change in position of the peak. Since the procedure involves fitting direct gaps in the band structure to the experimental values, we think that these direct transitions are accurate at the important points in the Brillouin zone. Indirect transitions are discussed in Section VI.

## IV InP Results

The band structure in the principal symmetry directions obtained from the optical data at 5°K for InP is shown in Fig. 3;the results are similar to energy band calculations[14] using the $\vec{k}\cdot\vec{p}$ method. Figs. 4, 5, 6 show our results for the calculated optical functions. Table 1 tabulates the important critical points.

The threshold in $\epsilon_2(\omega)$ (calculated energies referred to in this section correspond to structure in $\epsilon_2(\omega)$ unless otherwise noted) is caused by $\Gamma_{15} - \Gamma_1$ transitions at 1.50 eV. If spin-orbit corrections were included in our calculation, ($\Delta_0 = 0.21$ eV), we would obtain the following energy difference:

$$(\Gamma_8 - \Gamma_6) = (\Gamma_{15} - \Gamma_1) - \frac{1}{3}\Delta_0 = 1.43 \text{ eV}$$

in good agreement with the measured value[15] of 1.42 eV. The rise and peak in the region near 3.35 eV is caused by $L_3 - L_1$ transitions at 3.2 eV ($M_1$ and singularity)/$\Lambda_3 - \Lambda_1$ transitions near the point (0.3, 0.3, 0.3) at 3.22 eV ($M_1$ singularity). The main peak in the region of 4.9 eV is caused primarily by $\Sigma_2 - \Sigma_1$ transitions at (0.7, 0.7, 0.7) in the Brillouin zone (BZ) with an energy splitting of 5.02 eV ($M_2$ singularity). Some contribution comes from the 4.82 eV shoulder and these are attributed to $\Delta_5 - \Delta_1$ transitions at 4.7 eV ($M_0$ singularity) and $X_5 - X_1$ transitions at 4.71 eV ($M_1$ singularity). The small shoulder in the calculated $\epsilon_2(\omega)$ at 5.35 eV is caused by $X_5 - X_3$ 4-6 transitions having an energy difference of 5.29 eV ($M_0$ singularity); this structure does not appear in the $R(\omega)$ curve. The discontinuous structure in $\epsilon_2(\omega)$ at 5.6 eV arises from a volume effect for transitions between the 3rd and 6th bands near the point (0.3, 0.1, 0); the reflectivity structure is at 5.48 eV. The peak at 5.82 eV comes from $\Delta_5 - \Delta_1$ transitions near the point (0.7, 0, 0) ($M_1$ singularity). Finally the third prominent peak was caused by (4-6) transitions near L at 6.2 eV. Comparison of these last three structures with experiment is only fair.

The experimental reflectivity at 300°K is compared in Fig. 5 with our theoretical results for 5°K. The first peak after the small threshold structure

in the experimental curve is at 3 eV while we predict a peak at 3.30 eV; the experimental shoulder near 4.8 eV corresponds to the 4.75 eV theoretical shoulder. The main experimental peak at 5.05 eV has its counterpart in the 5.06 eV calculated peak. Experiment 2 shows a small shoulder at 5.6 eV which corresponds to the calculated shoulder at 5.48 eV; the larger shoulder at 5.6 eV has its theoretical counterpart in the small peak at 5.86 eV. The last structure recognized in our theoretical calculation is a broad peak at 6.47 eV and this corresponds to the 6.57 eV experimental value. Each of the experimental structures up to 6.7 eV has its theoretical counterpart. The agreement in magnitude is reasonably good when compared with Cardona's[17] data except for the first peak which can be interpreted as excitonic enhancement of the experimental curve in this energy region. The difference in position of the peaks is due to the temperature difference between the data used for our calculation and the temperature of the experimental reflectivity curves; the 300°K curves shift to lower energy as expected.

In Fig. 6 we show a comparison between the $R'(\omega)/R(\omega)$ theoretical curve and the modulated reflectivity of Fig. 2 at 5°K. In this curve the agreement in the positioning of the peaks is very good as shown in Table 1. Referring to these curves we make two remarks: (1) if spin-orbit effects were included, the 3.30 eV peak coming from the $\Lambda_3 - \Lambda_1$ band would split into two peaks at 3.23 eV and 3.37 eV ($\Delta_1 = 0.14$ eV) corresponding to the peak and shoulder at 3.24 eV and 3.38 eV in the experimental curve; (2) the small shoulder at 5.48 eV of the theoretical curve may be associated with the small structure at 5.5 eV of the experimental curve; the structure would be almost unnoticeable in the corresponding reflectivity curve.

## V GaP Results

In Fig. 7 we show a comparison between the calculated modulated reflectivity curve of Walter and Cohen[4] for GaP with the experimental results given in Sec. II. The calculations were done at an assumed temperature of 300°K. The calculated band structure, $\epsilon_2(\omega)$, and $R(\omega)$ for GaP also appear in Ref. 4. Identifications of the important reflectivity structure is tabulated in Table II. The positions of the important reflectivity peaks are given by those zeroes of $R'(\omega)/R(\omega)$ at which the slope is negative. The other structure appearing in the derivative spectrum is much finer; some of the details are practically imperceptible when seen in the normal reflectivity spectrum.

The fundamental gap in GaP is the indirect $\Gamma_{15} - X_1$ gap. The calculated value is 2.19 eV and the experimental value is 2.22 eV, as determined by absorption and recombination radiation experiments.[18] The smallest direct gap occurs at $\Gamma$ at 2.79 eV for theory and at 2.78 eV for experiment. The major structure in the 3.4 - 3.9 eV region is a reflectivity peak centered at 3.68 eV caused by $\Lambda(4\text{-}5)$ and $\Lambda(3\text{-}5)$ transitions. The theoretical peak in the reflectivity occurs at 3.70 eV, giving excellent agreement with experiment. The next major reflectivity peak occurs at 5.31 eV in the experimental measurements and at 5.3 eV in the theoretical calculations. This peak is caused by a combination of $\Sigma(4\text{-}5)$, $\Delta(3\text{-}5)$, and $\Delta(4\text{-}5)$ transitions, all with large oscillator strengths. The fine structure in this region consists of a reflectivity shoulder at 4.74 eV caused by $\Delta(4\text{-}5)$ and $X(4\text{-}5)$ transitions. This shoulder occurs in the calculated reflectivity at about 4.7 eV.

## VI Indirect Gaps

For GaP as well as InP we have obtained a very good agreement between measured and calculated reflectivity and modulated reflectivity. The fitting is good enough to indicate that our identifications of the important direct transitions in the reflectivity experiments are correct and that our band structure is accurate with respect to direct transitions.

In GaP the minimum gap is the indirect $\Gamma_{15} - X_1$ gap. This transition has been determined experimentally by absorption and recombination radiation experiments[18] and it is found to be 2.22 eV while our calculated value is 2.19 eV; in these experiments Zallen and Paul also determine the pressure dependence of this gap and of the $\Gamma_{15} - \Gamma_1$ direct gap (the experimental value of the $\Gamma_{15} - \Gamma_1$ being 2.78 eV in agreement with the calculated value of 2.75 eV). The measured pressure coefficients are $dE(\Gamma_{15} - \Gamma_1)/dP = 10.7 \pm 10\% \times 10^{-6}$ eV/bar and $dE(\Gamma_{15} - X_1)/dP = -1.1 \pm 10\% \times 10^{-6}$ eV/bar. We have calculated the pressure coefficients for these gaps; our results are as follows:

$$dE(\Gamma_{15} - \Gamma_1)/dP = 12.6 \times 10^{-6} \text{eV/bar}; \quad dE(\Gamma_{15} - X_1)/dP = -1.0 \times 10^{-6} \text{ eV/bar}$$

in good agreement with the experimental values. The calculation involves the evaluation of the change in energy levels with small changes in lattice constant (the pseudopotential was scaled[1] for the volume change). The measured compressibility was also used in the calculation.

For InP a direct measurement of the $\Gamma - X$ indirect transition has not been performed. One possibility for obtaining this value arises from what Paul[18] calls "the empirical rule" which says that all the gaps in III-V and II-VI

semiconductors have roughly the same pressure dependence. The pressure coefficient of the direct gap between the $\Gamma_{15}$ valence band and the $\Gamma_1$ conduction band is of the order of $10 \times 10^{-6}$ eV/bar and the pressure coefficient of the $\Gamma_{15} - X_1$ indirect gap is roughly $-1 \times 10^{-6}$ eV/bar. Our calculated values for this crystal are:

$$dE(\Gamma_{15} - \Gamma_1)/dP = 8.4 \times 10^{-6} \text{ eV/bar} \; ; \quad dE(\Gamma_{15} - X_1)/dP = -1.3 \times 10^{-6} \text{ eV/bar} \; .$$

At sufficiently high pressure (> 50 k bar) the indirect $\Gamma_{15} - X_1$ gap will become the smallest gap and therefore directly observable.

Another possibility is explored by Hakki et al[5]; in these experiments they combine pressure and composition dependence on In-GaP alloys. Using Paul's "empirical rule" they are able to identify the smallest gap for a given composition as a function of pressure; then from extrapolation, they determine the variation with composition of the $\Gamma_{15} - X_1$ gap at zero pressure. A linear extrapolation of the $\Gamma_{15} - X_1$ gap to the InP side gives a value of 2 eV. The extrapolated pressure coefficient for this gap is $-1.1 \times 10^{-6}$ eV/bar. We think that the conclusions of Hakki et al are correct; our calculated value for this gap at $5^{\circ}$K is 2.84 eV. To compare the band structure calculation with experiment for the indirect gaps, we have introduced a $k^2$ dependent term in our band structure as shown by the dotted line in Fig. 3. The expression used is $E(\vec{k}) = E_{EPM}(\vec{k}) - \gamma k^2$; $\gamma$ is adjusted to give the experimentally determined $\Gamma_{15} - X_1$ gap, and its value is $\gamma = 0.743$ ev $\text{Å}^2$. Writing $-\gamma = \hbar^2/2m'$ and $1/m^* = 1/m' + 1/m_e$, we find that our correction may be thought of as a mass renormalization with $m^* = 1.22\ m_e$.

## Acknowledgement

Part of this work was done under the auspices of the U. S. Atomic Energy Commission.

## References

1. M. L. Cohen and V. Heine, Solid state physics 24, edited by H. Ehrenreich, F. Seitz and D. Turnbull (Academic Press, Inc., New York, N. Y. (1970).)
2. J. P. Walter and M. L. Cohen, Phys. Rev. B4, 1877 (1971).
3. J. P. Walter and M. L. Cohen, Phys. Rev. B1, 2661 (1970).
4. J. P. Walter and M. L. Cohen, Phys. Rev. 183, 763 (1969).
5. B. W. Hakki, A. Jayaraman, and C. K. Kim, J. Appl. Phys. 41, 5291 (1970).
6. R. R. L. Zucca and Y. R. Shen, Phys. Rev. B1, 2668 (1970).
7. M. Cardona, J. Appl. Phys. Suppl. 32, 2151 (1961).
8. H. C. Gatos and M. C. Levine, Prog. in Semiconductors 9, 3 (1965).
9. E. Matatagui, A. G. Thompson, and M. Cardona, Phys. Rev. 176, 950 (1968).
10. A. G. Thompson, M. Cardona, K. L. Shaklee, and J. C. Woolley, Phys. Rev. 146, 601 (1966).
11. M. Cardona, K. L. Shaklee, and F. Pollak, Phys. Rev. 154, 696 (1967).
12. K. L. Shaklee and J. E. Rowe, Applied Optics 9, 627 (1970).
13. M. L. Cohen and T. K. Bergstresser, Phys. Rev. 141, 789 (1970).
14. F. H. Pollak, C. W. Higginbotham and M. Cardona, J. Phys. Soc. Japan Suppl. 21, 1966.
15. W. J. Turner, W. E. Reese and G. D. Pettit, Phys. Rev. 136, A1467 (1964).

16. J. C. Woolley, and S. S. Vishnubhatla, Canad. J. Phys. 46, 1769 (1968).

17. M. Cardona in Semiconductors and semimetals, Vol. 3, R. W. Willardson and A. C. Beer, eds., Academic Press, New York, 1967, p. 138.

18. R. Zallen and W. Paul, Phys. Rev. 134, A1628 (1964).

19. W. Paul in Les proprietes physiques des solides sous pression, Colloques Internationaux du Centre National de la Recherche Scientifique, Grenoble, 1969, p. 199.

## Figure Captions

Fig. 1 Experimental modulated reflectivity for InP at 5 , 77 and 300°K.

Fig. 2 Experimental modulated reflectivity for GaP at 5 , 77 and 300°K.

Fig. 3 Electronic band structure of InP along the principal symmetry directions in the Brillouin zone. The dotted line represents the corrected band structure $E(k) = E_{EPM}(k) - \gamma k^2$.

Fig. 4 Calculation of the imaginary part of the frequency dependent dielectric function for InP.

Fig. 5 Calculated and measured reflectivity for InP. Experiment 1 is M. Cardona in Semiconductors and semimetals, Vol. 3, R. W. Willardson and A. C. Beer, eds., Academic Press, N.Y., 1967, p. 138; experiment 2 is S. S. Vishnubhatla and J. C. Wooley, Canad. J. Phys. 46, 1769 (1968); experiment 3 is present work.

Fig. 6 Comparison of the theoretical and experimental modulated reflectivity spectrum for InP. Experimental curve is at 5°K.

Fig. 7 Comparison of the theoretical (J. P. Walter and M. L. Cohen, Phys. Rev. 183, 763 (1970)) and experimental modulated reflectivity spectrum for GaP. Experimental curve is at 300°K.

## Table Captions

Table 1 Identification of transitions responsible for the prominent theoretical and experimental reflectivity structure in InP, including location in the Brillouin zone, energy, and symmetry of calculated critical points (cp).

Table 2 Identification of transitions responsible for the prominent theoretical and experimental reflectivity structure in GaP, including location in the Brillouin zone, energy and symmetry of calculated critical points (cp).

Table 1 InP Reflectivity structure[a]

| Theory | Experiment | Location in zone | Symmetry | $c_p$ energy |
|---|---|---|---|---|
| 1.43 eV[b] | 1.42 eV[c] | $\Gamma$(4-5)(0,0,0) | $M_0$ | 1.5 eV |
| 3.23[b] | 3.24 | L(4-5)(0.5,0.5,0.5) | $M_0$ | 3.2 |
| 3.37[b] | 3.38 | $\Lambda$(4-5)(0.3,0.3,0.3) | $M_1$ | 3.22 |
| 4.75 | 4.78 | $\Delta$(4-5)(0.8,0,0) | $M_0$ | 4.7 |
| | | X(4-5)(1.0,0,0) | $M_1$ | 4.71 |
| | | Volume near (4-5)(0.3,0,0) | - | 4.88 |
| 5.06 | 5.10 (5.05) | $\Sigma$(4-5)(0.7,0.7,0) | $M_2$ | 5.02 |
| 5.48 | (5.25) | Vol.(3-6)(0.3,0.1,0) | - | 5.5 |
| 5.86 | 5.77(5.6) | $\Delta$(4-6)(0.7,0,0) | $M_1$ | 5.77 |
| 6.47 | (6.57) | L(4-6)(0.5,0.5,0.5) | $M_0$ | 6.2 |
| | | $\Lambda$(4-6)(0.4,0.4,0.4) | $M_1$ | 6.28 |

(a) Data in parentheses from Woolley-Vishnubhatla, Canad. J. Phys. 46, 1769 (1968). Other data from this paper's 5°K experiment.

(b) Corrected to include spin-orbit corrections.

(c) W. J. Turner, W. E. Reese and G. D. Pettit, Phys. Rev. 136, A1467 (1964).

Table 2 GaP Reflectivity structure

| Theory | Experiment | Location in zone | Symmetry | $c_p$ energy |
|---|---|---|---|---|
| 2.79 eV | 2.78 eV | $\Gamma(4\text{-}5)(0,0,0)$ | $M_0$ | 2.79 eV |
| | 2.86 | | | |
| 3.70 | 3.69 | $L(4\text{-}5)(0.5,0.5,0.5)$ | $M_0$ | 3.40 |
| | | $\Lambda(4\text{-}5)(0.15,0.15,0.15)$ | $M_1$ | 3.76 |
| 4.7 | 4.74 | $\Delta(4\text{-}5)(0.71,0,0)$ | $M_0$ | 4.50 |
| | | $X(4\text{-}5)(1,0,0)$ | $M_1$ | 4.57 |
| 5.3 | 5.31 | $\Delta(4\text{-}5)(0.30,0,0)$ | $M_3$ | 4.72 |
| | | $\Sigma(4\text{-}5)(0.50,0.50,0)$ | $M_2$ | 5.20 |

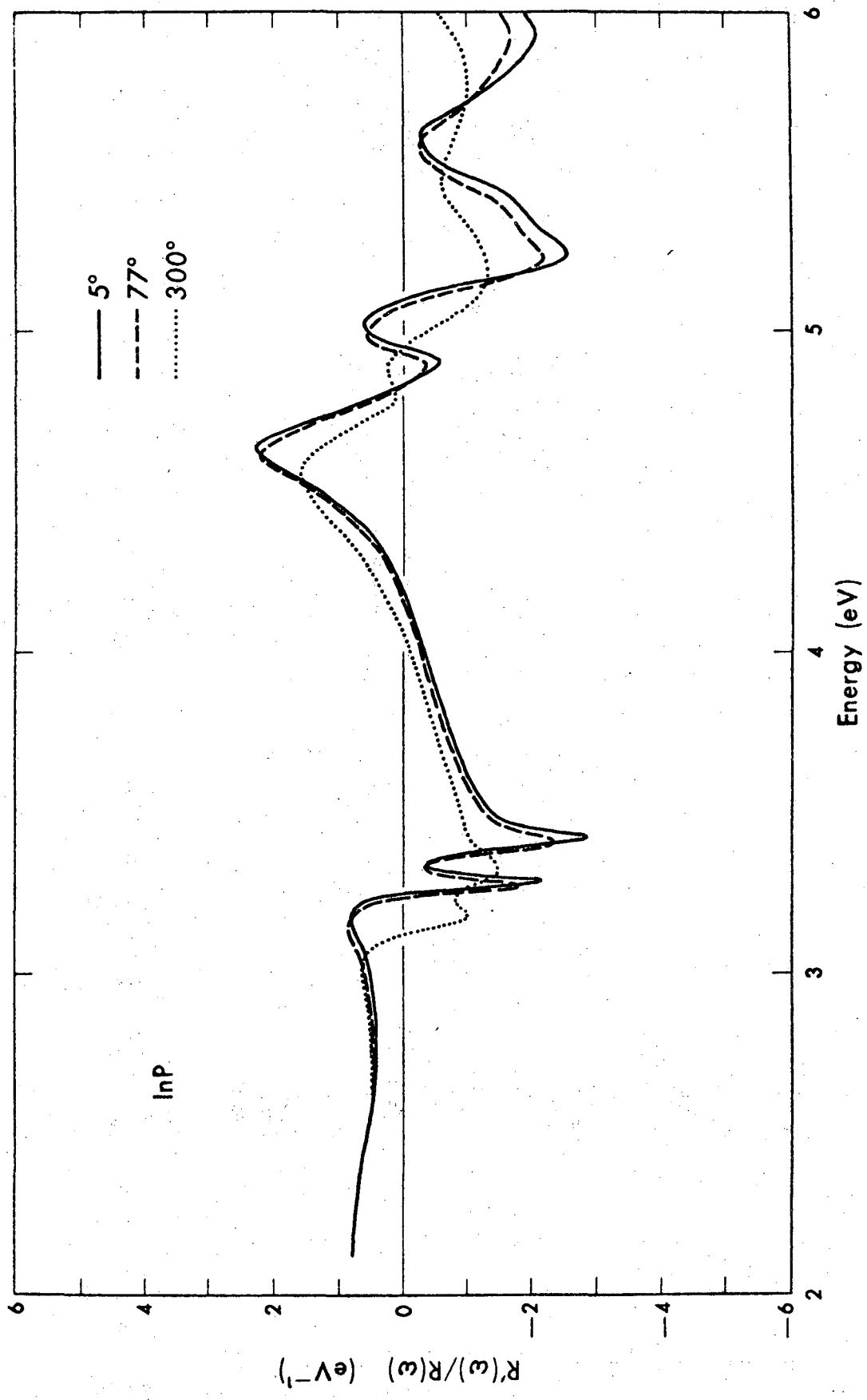


Fig. 1

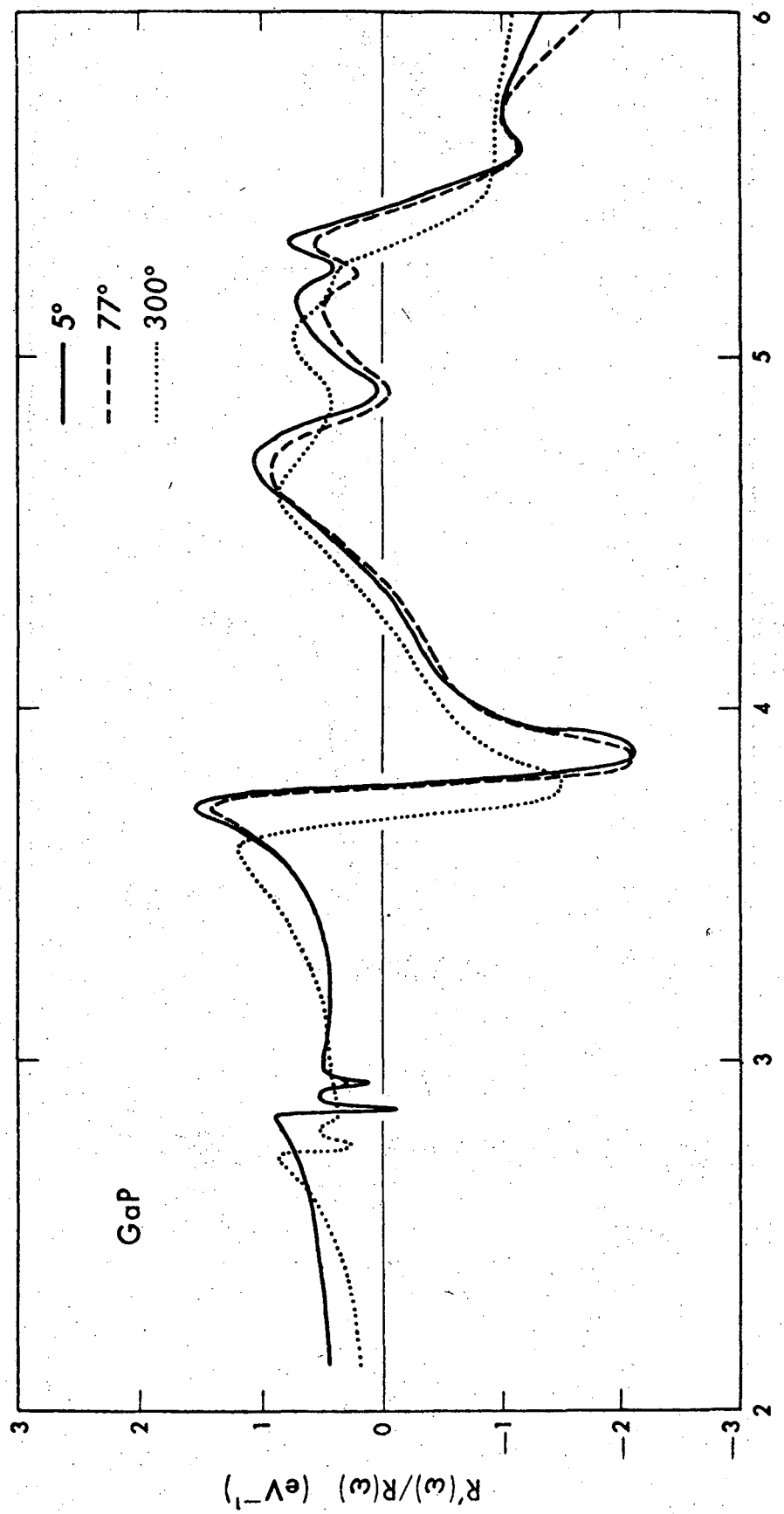


Fig. 2

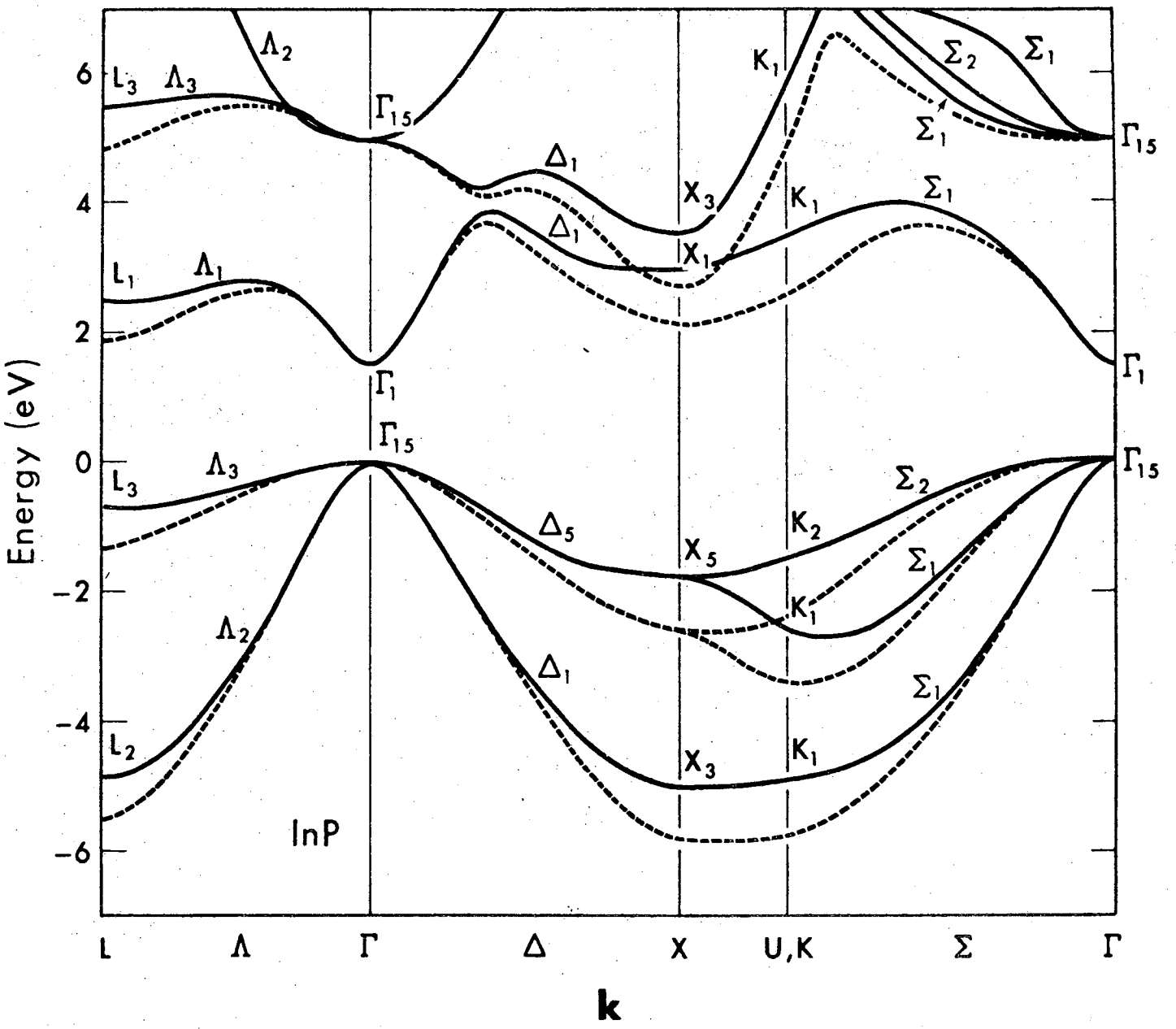
Energy (eV)
6
4
2
0
-2
-4
-6
InP
L
Λ
Γ
Δ
X
U,K
Σ
Γ
k
L3
Λ3
Λ2
Γ15
Δ1
X3
K1
Σ2
Σ1
L1
Λ1
Γ1
X1
K1
L3
Λ3
Γ15
Δ5
X5
K2
Σ2
Σ1
K1
Λ2
Δ1
Σ1
L2
X3
K1

Fig. 3

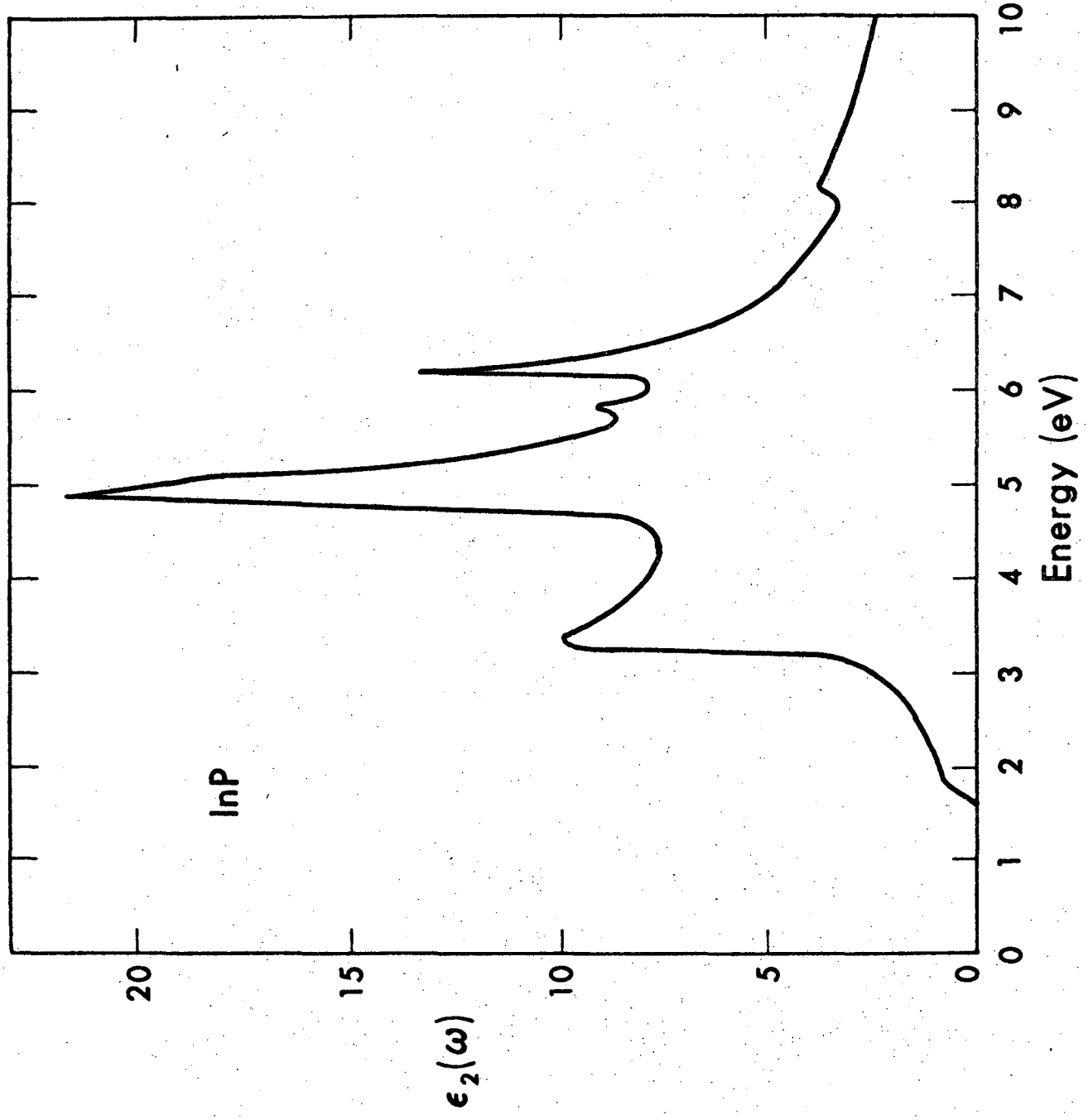


Fig. 4

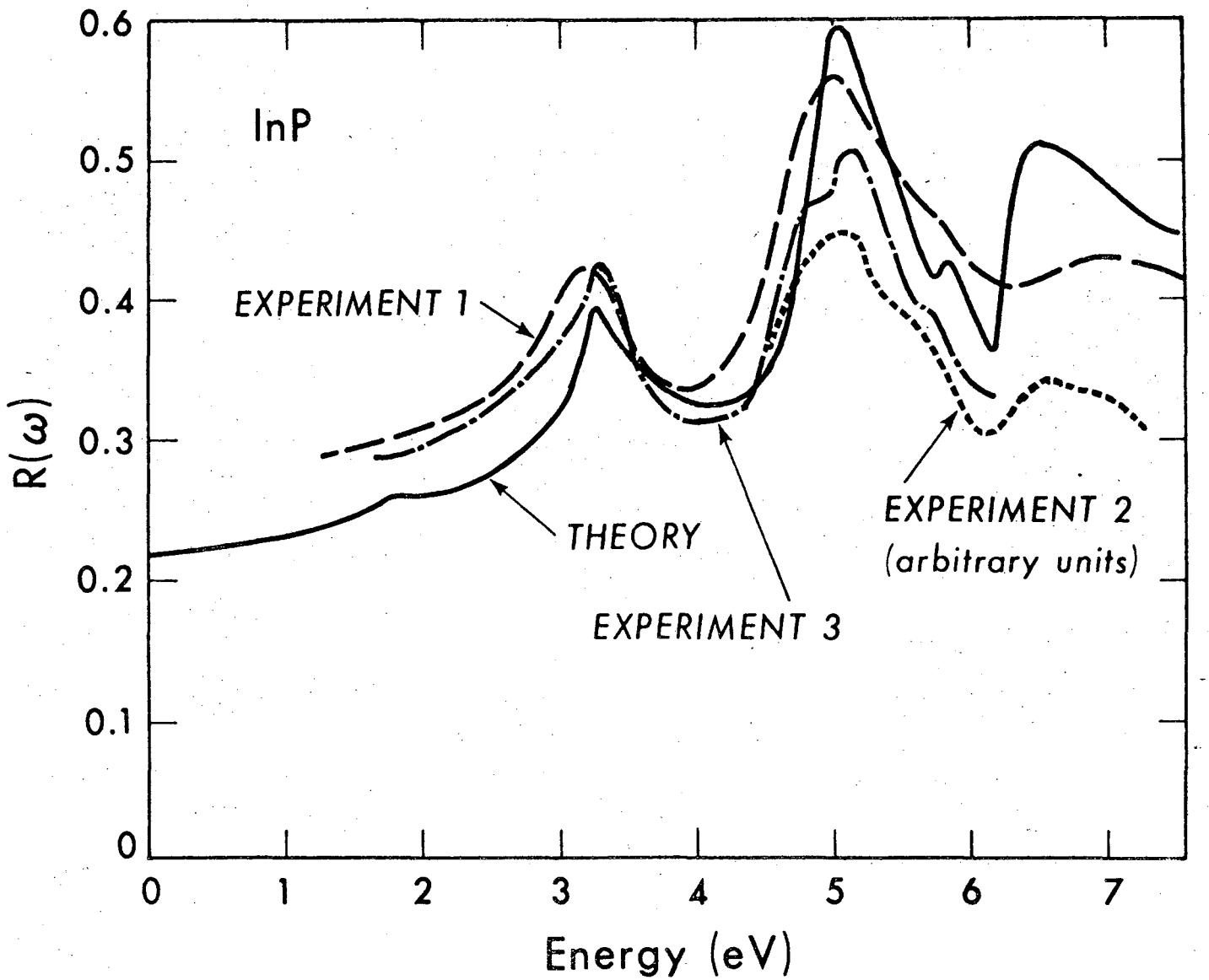
InP
EXPERIMENT 1
THEORY
EXPERIMENT 3
EXPERIMENT 2
(arbitrary units)
R(ω)
Energy (eV)
0.6
0.5
0.4
0.3
0.2
0.1
0
0
1
2
3
4
5
6
7

Fig. 5

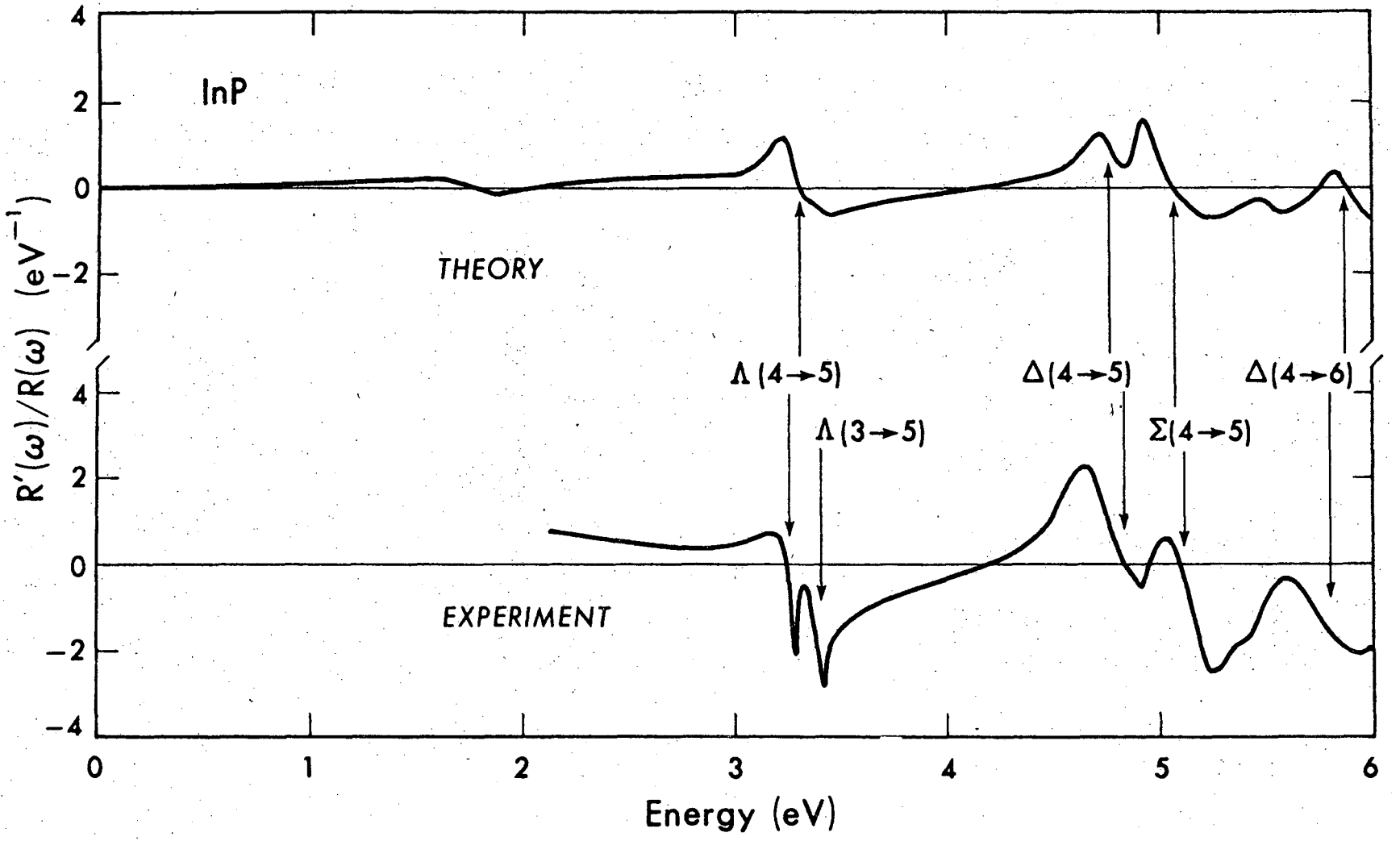
InP
THEORY
EXPERIMENT
Λ(4→5)
Λ(3→5)
Δ(4→5)
Σ(4→5)
Δ(4→6)
R'(ω)/R(ω) (eV⁻¹)
Energy (eV)
4
2
0
−2
−4
0
1
2
3
4
5
6

Fig. 6



LBL-479

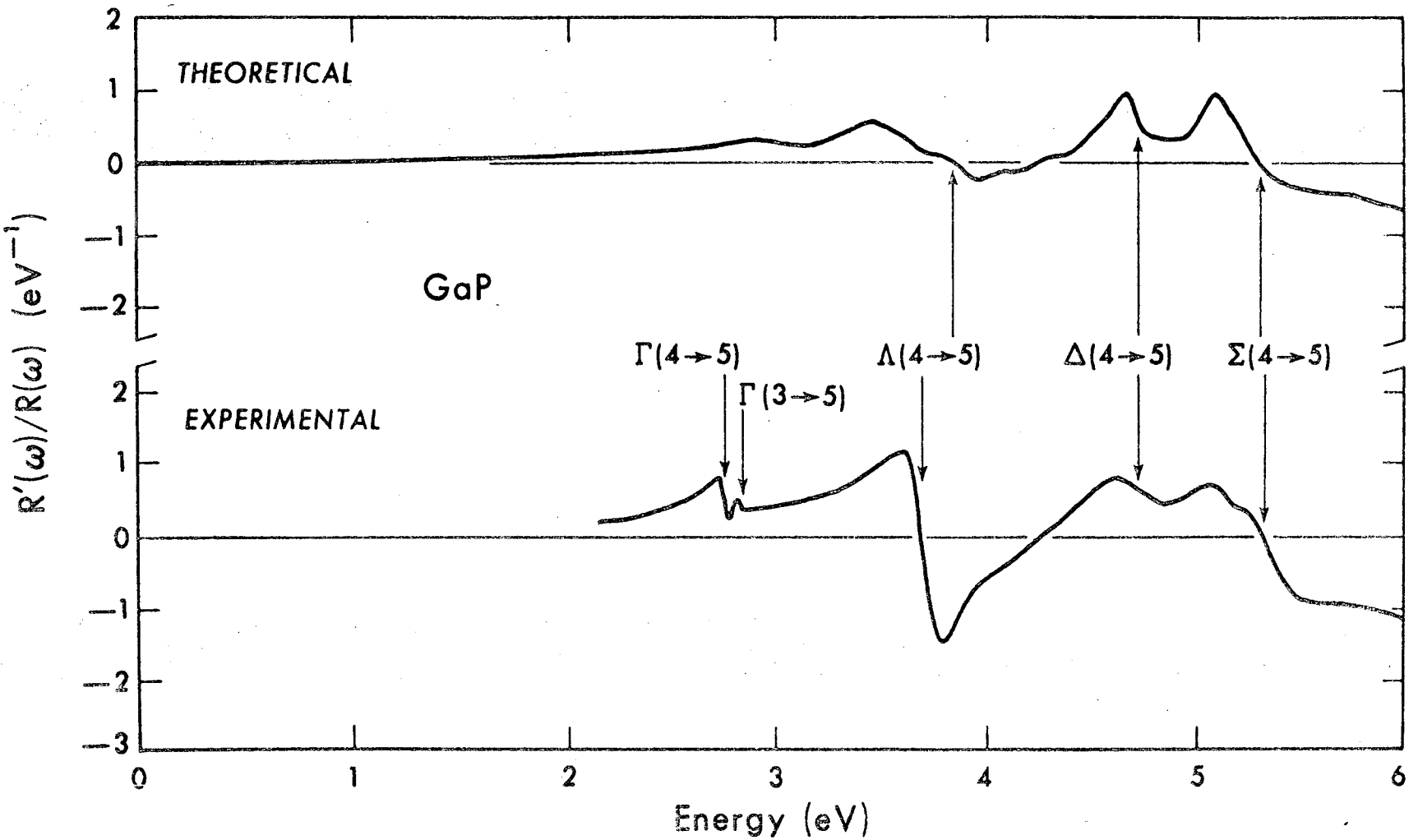
THEORETICAL
GaP
EXPERIMENTAL
Γ(4→5)
Γ(3→5)
Λ(4→5)
Δ(4→5)
Σ(4→5)
R'(ω)/R(ω) (eV⁻¹)
Energy (eV)
2
1
0
−1
−2
−3
0
1
2
3
4
5
6

Fig. 7

*TECHNICAL INFORMATION DIVISION*
*LAWRENCE BERKELEY LABORATORY*
*UNIVERSITY OF CALIFORNIA*
*BERKELEY, CALIFORNIA 94720*